Using Probabilistic Analysis with Finite Element Modeling of High Temperature Geothermal Well Casings

Conference Paper · October 2013

4 authors:


Gunnar Skúlason Kaldal
University of Iceland


Magnus Jonsson
University of Iceland


Halldór Pálsson
University of Iceland


Sigrun Nanna Karlsdottir
University of Iceland

Using Probabilistic Analysis with Finite Element Modeling of High Temperature Geothermal Well Casings

Gunnar Skúlason Kaldal [*], Magnús Þór Jónsson, Halldór Pálsson, and Sigrún Nanna Karlsdóttir

Faculty of Industrial Engineering, Mechanical Engineering and Computer Science, University of Iceland, Hjarðarhagi 2-6, 107 Reykjavík, Iceland

Abstract

High temperature geothermal wells which are drilled in geothermal areas are constructed of several concentric steel casings that are cemented together. The structural integrity of such well casings is essential for the utilization of high temperature geothermal wells. The temperature change in high temperature geothermal wells is large and much larger than commonly seen in oil wells. This large temperature change can cause problems in the casing due to thermal expansion of materials. The wellhead rises during discharge due to thermal expansion of the steel in the casing and the large temperature change can also lead to casing collapse due to expanding annular fluids. With recent increasing interest in drilling deeper geothermal wells the strength of the casing becomes one of the most limiting factor. A nonlinear structural finite element model of the cased well is presented and discussed here. The purpose of the model is to evaluate the structural integrity of the casing when it is subjected to thermo-mechanical loads. The outcome of the model depends highly on the accuracy of the input parameters, i.e. geometrical sizes and material properties. The accuracy of the results are evaluated with the use of probabilistic design analysis where selected input parameters of the model are assumed to contain a reasonable amount of scatter. The uncertainties of the model can thus be quantified.

1. Introduction

Geothermal wells are constructed of several concentric steel casings which are fully cemented together and cemented to the rock formation. Usually, three casings are used; the production casing, anchor casing and surface casing. The wellhead consists of a casing head flange, expansion spool and a master valve. The wellhead is attached to the top of the anchor casing and the production casing movements relative to the anchor casing is accommodated below the master valve inside the expansion spool [5].

During the discharge of high temperature geothermal wells, the temperature difference in the well from non-flowing to flowing conditions is large. To take an example, reservoir temperatures in the Krafla high temperature geothermal area in Iceland typically range from $210\,^{\circ}\mathrm{C}$ to $350\,^{\circ}\mathrm{C}$ [11]. The large temperature change generates thermal stress in the casing which is partially constrained by the concrete. While the well warms up the wellhead rises as a result of thermal expansion of the casings and concrete. Casing failures can lead to a reduced energy output from the well, render it inoperative and in worst cases cause unsafe conditions above the surface. Thus the structural integrity of well casings is essential for the utilization of high temperature geothermal wells.

The casings and the wellhead form a structural system which is unpractical to solve analytically mainly due to the nonlinear behavior of the contacting surfaces. Therefore, the structural system is analyzed numerically with the use of the nonlinear finite element method (FEM). A thermal and nonlinear structural model of the cased well is constructed where nonlinearities, e.g. friction, plasticity and large non-uniform deformations are accounted for. The nonlinear axi-symmetric model described here is a continuation of the work described by Kaldal [7]. Other models of geothermal wells have been created, e.g. an elastic 2D FEM model presented by Gretarsdottir [4] and a nonlinear FEM model by Magnusdottir where the bonding characteristics between the production casing and its outer concrete were analyzed [10]. The collapse of

*gunnarsk@hi.is

the production casing is a non-symmetrical phenomenon which cannot be analyzed with this model but has been modeled with nonlinear 3D FEM models by Kaldal [6][8].

As opposed to deterministic analysis, where input parameters are treated as constants which results in a one possible solution, a probabilistic approach is used, where the input parameters are assumed to contain a reasonable amount of scatter, which then gives an estimate of the model uncertainties. Here, selected results from the FEM model are used as outputs for the probabilistic analysis. Scatter plots of the input parameters versus the output results reveal which input parameters are significant to the results of the FEM model. A cumulative distribution function of the wellhead movement and the maximum von Mises stress in the casings and surrounding concrete is obtained here and are used to review the uncertainty of the model. In this paper, probabilistic analysis of the FEM model is presented where several input parameters are evaluated.

2. Probabilistic design

Probabilistic design is an analysis technique for assessing the effect of uncertain input parameters and model assumptions [1]. Using this method the uncertainties of the model can be quantified by acknowledging that the input parameters are not constants but rather parameters that follow statistical distribution functions such as Gaussian or normal distribution. By this assumption the limited outcome of deterministic results is avoided and the uncertainties in the model and probability distribution of the results are analyzed. Of course, the modeling error which refers to the difference between the physical system and its mathematical model [2] can be larger due to numerous approximations made to the geometry, material properties, load, etc. But all in all this method gives a map of the results rather than one point.

Intertwined in the method is the determination of the sensitivity of individual parameters to the results. For the model described below, each input parameter is assumed to follow normal distribution given by assumed mean and standard deviation. The probabilistic analysis employs the Monte Carlo Simulation method with Latin Hypercube Sampling, which avoids repeated samples [1]. A given number of simulation loops are performed and before each loop, individual input parameter is randomly given a value within its normal distribution domain. When the simulation loops are finished the sensitivity of the input parameters to the results can be visualized with scatter plots.

For the probabilistic analysis used on the FEM model described below, 400 simulation loops were used. The selected input parameters that were used for the probabilistic analysis are listed in Table 1. Their assumed means and standard deviation are listed as well. The standard deviation σ provides the sample range for the parameter and 99.7% of the samples should fall within 3σ from the mean provided that the number of simulation loops is sufficient.

Table 1: Probabilistic design input parameters (mean and assumed standard deviation).

Parameter	Units	Mean	Std
μ	-	0.45	0.15
τ_{max}	MPa	0.46	0.13
E_{co}	GPa	2.4	0.6
E_{gr}	GPa	80	20
f_c	MPa	30	7.5
ρ_{st}	$^{\mathrm{kg}}/_{\mathrm{m}^3}$	6125	150
ρ_{co}	$^{\mathrm{kg}}/_{\mathrm{m}^3}$	1600	200
α_{st}	$^{1}/_{^\circ\mathrm{C}}$	12e-6	1e-6
α_{co}	$^{1}/_{^\circ\mathrm{C}}$	10e-6	1.5e-6
σ-ϵ_{sc}	-	1	0.1

3. FEM model description

A nonlinear thermal and structural model of a high temperature geothermal well which reaches from the wellhead to the bottom of the production casing is constructed with the use of the finite-element method (FEM). The focus is to analyze the structural system which consists of a wellhead and several concentric casings connected together and to the formation with concrete. The model is two dimensional and axisymmetric around the center of the well. It includes nonlinearities which are found in large geometrical displacements, in material properties and in connectivity between contacting surfaces.

The model, shown in Figure 1, is parametrically designed so geometrical sizes and material properties are adjustable by the user. Simplified couplings with no threads are included in the production casing to account for the anchoring effect of the couplings in the concrete. A simplified wellhead based on an actual design is also included to account for pressure loads and the interaction between the casing and the wellhead. Material properties and reference values that are used in the model are listed in Table 2. Additionally, the reference value for the coefficient of friction between steel and concrete is $\mu = 0.5$ and

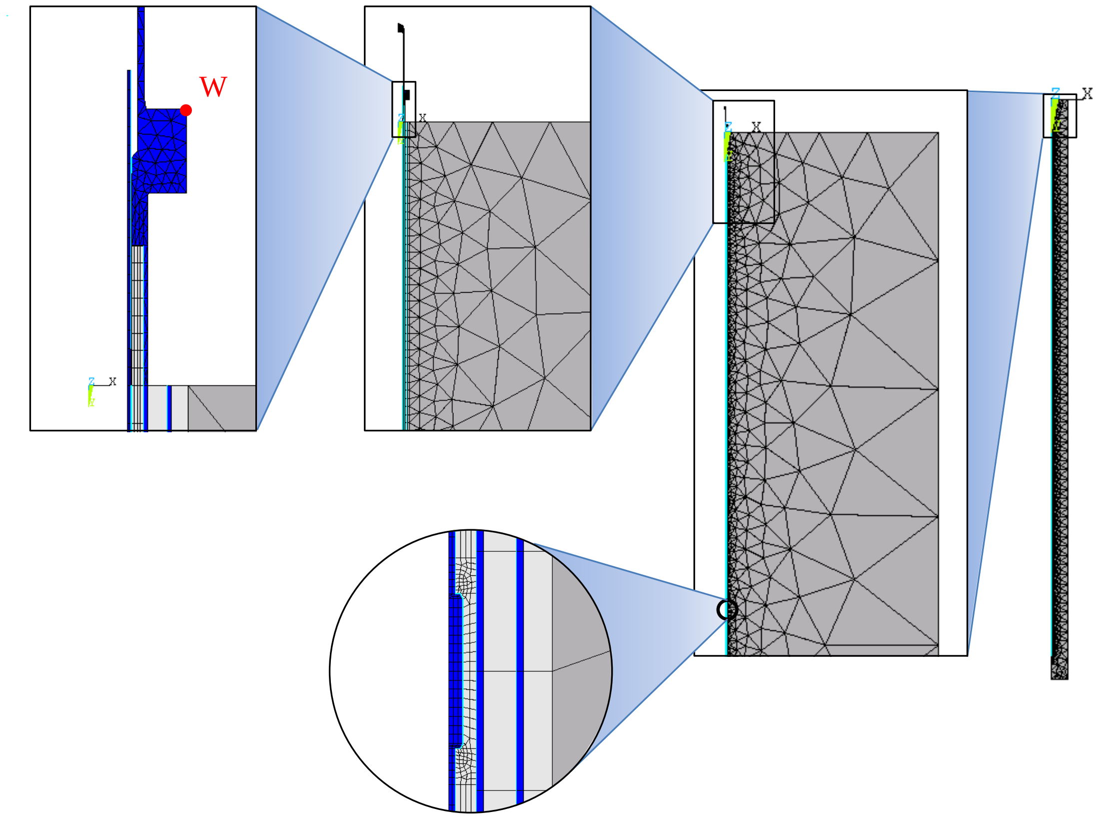

Figure 1: The geometry of the model.

the maximum shear stress when sliding initiates is $\tau_{max} = 0.46\,\text{MPa}$. Nonlinear material properties of steel grades K55, L80, T95 and X56 are implemented in the model with the use of stress-strain curves which were obtained from tensile tests [9]. The concrete is assumed to yield plastically above its maximum compressive strength and the formation is assumed to be solid basaltic rock.

Table 2: Material properties and numerical values used in the model.

Material property	Units	Steel	Concrete
Young's modulus (E)	GPa	210	2.4
Poisson's ratio (ν)	-	0.3	0.15
Density (ρ)	$^{kg}/_{m^3}$	7850	1600
Th. conductivity (K)	$^{W}/_{m^\circ C}$	50	0.81
Specific heat (c)	$^{J}/_{kg^\circ C}$	400	880
Th. expansion (α)	$^{1}/_{^\circ C}$	12e-6	10e-6
Compressive strength (f_C)	MPa	-	25e6

The frictional connection between surfaces in particular makes the model computationally complex. Contact element pairs are used between contacting surfaces. Their main purpose is to prevent surfaces to intersect each other, while still allowing gap formation and tangential movement between casings and concrete. The Coulomb friction model is used to describe friction between contacting surfaces, where it can withstand shear stresses up to a certain magnitude across its interface before they start sliding relative to each other [1]. Once the equivalent shear stress exceeds τ_{max} relative sliding begins. The Coulomb friction model is defined as:

$$\tau = \begin{cases} \mu P + b & \text{if } \tau < \tau_{max} \\ \tau_{max} & \text{if } \tau \geq \tau_{max} \end{cases} \tag{1}$$

where τ is the equivalent shear stress, τ_{max} is the maximum shear stress, μ is the isotropic coefficient of friction, b is the contact cohesion and P is the contact normal pressure, see Figure 2 for the graphical interpretation of the Coulomb friction model.

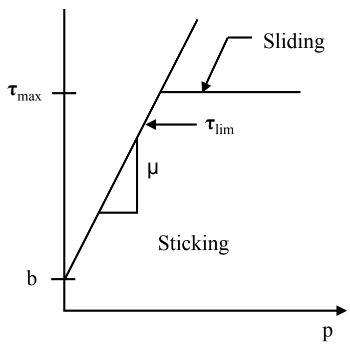

Figure 2: The Coulomb friction model in Ansys [1].

The boundary conditions of the model are defined such that no displacements are allowed in the lower and outer boundary of the model. The lower boundary is located 20 m deeper than the production casing shoe and the outer (radial) boundary of the rock formation is 20 m outward from the well, which is sufficient for both the thermal and the structural parts of the model. The wellhead movement is observed at the nodal point denoted with W on Figure 1.

4. Results

4.1. FEM results from a single simulation run

FEM results from a single simulation run, with the material properties values listed in Table 2, are presented here.

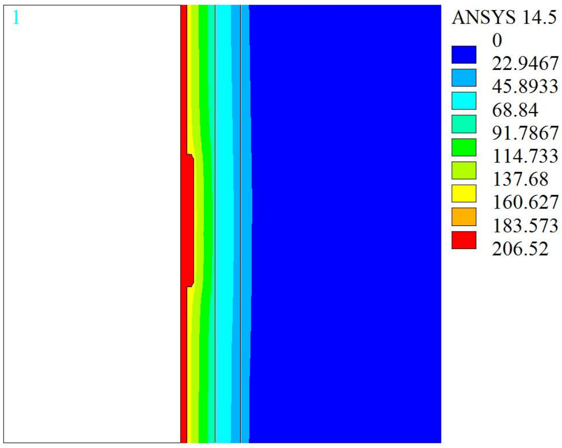

Figure 3: Temperature distribution 2.5 hours after discharge (°C).

The calculated temperature distribution at the top of the well 2.5 hours after discharge, which will be the reference time of the subsequent results, is displayed in Figure 3. A temperature change of 200 °C is assumed. The displacement at the top of the well is displayed in Figure 4. In this run the displacement of the production casing is 35.8 mm and the wellhead displacement is 11.7 mm. Stress concentration near the couplings of the casing is illustrated in Figure 5 where the maximum stress in the steel is produced near the couplings and in Figure 6 where the maximum stress in the concrete forms at the top of the couplings. In this case the maximum stress for both the concrete and the casing is formed at the second highest coupling.

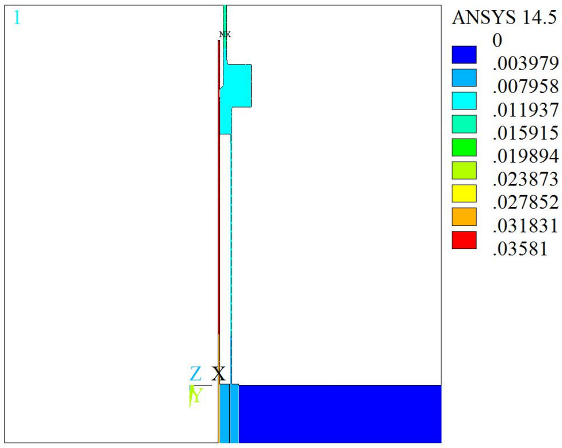

Figure 4: Displacement of the wellhead 2.5 hours after discharge (m). The displacement of the production casing is 35.8 mm and the wellhead displacement is 11.7 mm.

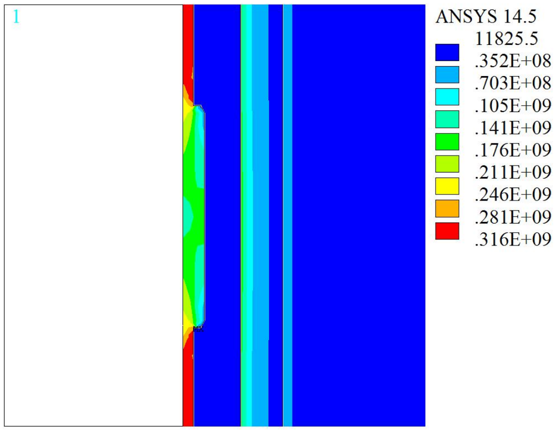

Figure 5: Von Mises stress at the second highest coupling (Pa).

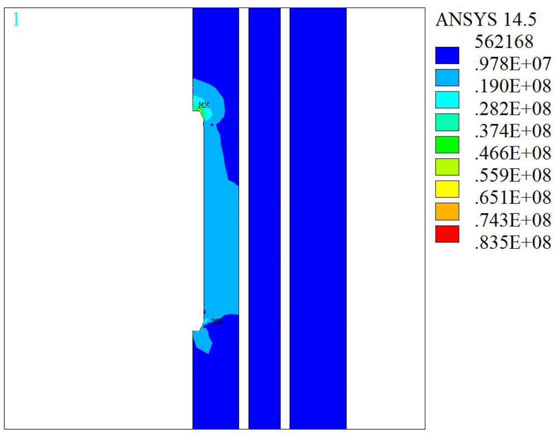

Figure 6: Von Mises stress of concrete at the second highest coupling (Pa).

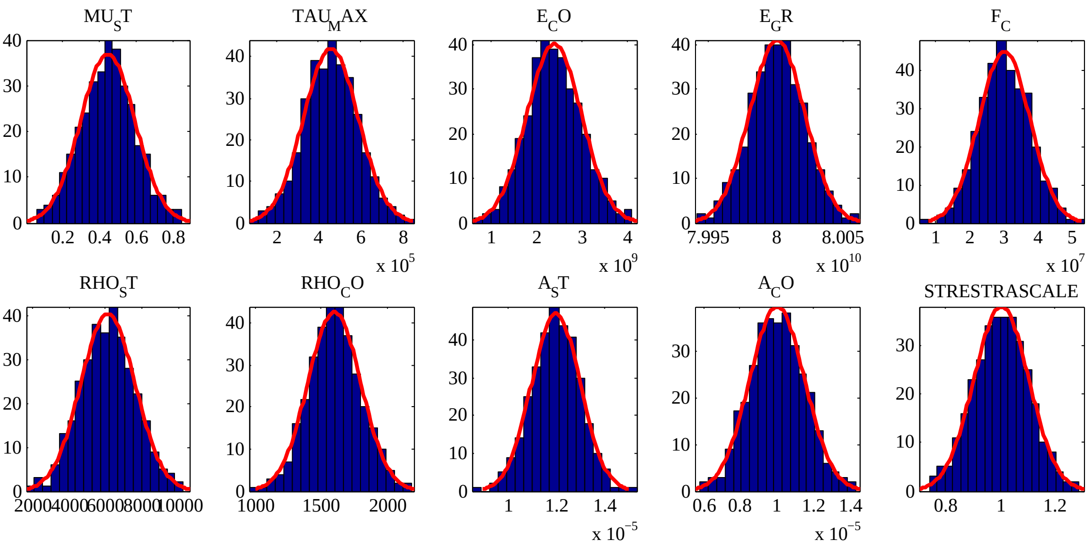

Figure 7: Histograms of normally distributed input parameters.

4.2. Distribution of inputs and outputs

The material properties for the FEM model that were selected as input parameters for the probabilistic analysis are listed in Table 1. Histograms of the input parameters which were assumed to follow normal distribution are seen in Figure 7. The samples of the input parameters follow normal distribution which confirms that for the probabilistic analysis, 400 Monte Carlo simulation loops are sufficient.

The results from the FEM model that were selected as outputs for the probabilistic analysis, i.e. wellhead displacement and maximum von Mises stress in the production casing, the anchor casing and the surrounding concrete for each casing, are displayed in the histograms in Figure 8 and discussed in the discussion section below.

4.3. Correlation between inputs and outputs

Scatter plots showing the correlation between the selected input parameters and the selected outputs of the model are illustrated in Figure 14. A significance level of the correlation between input and outputs is chosen to be 2.5%, so that $R^2 < 0.025$ is dismissed as insignificant.
For the first column, the wellhead displacement, the significant parameters are; μ_{st}, τ_{max} and α_{st} with correlations of $R^2 = 0.02528$, $R^2 = 0.32987$ and $R^2 = 0.35066$. All other input parameters are of no significance to the wellhead movement. Summary of the significant parameters and correlations is listed in Table 3.

Table 3: Significant input parameters and correlation with the results.

Output	Input	R^2
Wellhead displacement	μ_{st}	0.02528
	τ_{max}	0.32987
	α_{st}	0.35066
Max. von Mises stress of the production casing	α_{st}	0.36826
	σ-ϵ_{sc}	0.73963
Max. von Mises stress of the production concrete	τ_{max}	0.62363
	E_{co}	0.15270
	f_c	0.03274
	α_{st}	0.09283
	σ-ϵ_{sc}	0.02940
Max. von Mises stress of the anchor casing	ρ_{st}	0.02701
	ρ_{co}	0.21588
	α_{st}	0.73663
Max. von Mises stress of the anchor concrete	E_{co}	0.83435
	α_{st}	0.11622

4.4. Cumulative distribution function

If the results from all the Monte Carlo simulations are sorted and plotted against the proportion of the result values an empirical cumulative distribution function (CDF) of the results is obtained. These plotted curves can then be used to visualize the results. From the wellhead displacement results for example, seen in Figure 9, it can be stated with 90% certainty that the wellhead displacement is less than or equal to

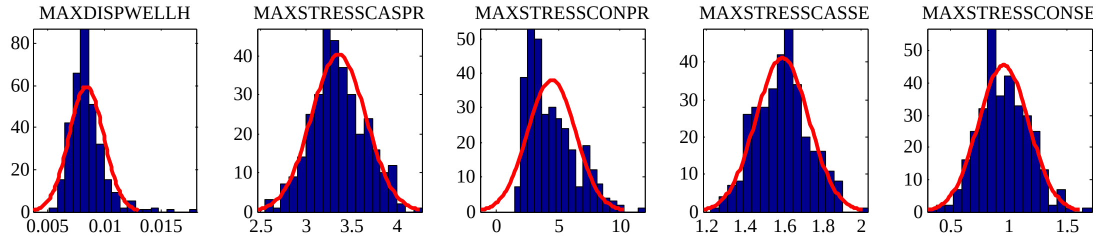

Figure 8: Histograms of the selected output results from the probabilistic analysis.

10 mm, with 95% certainty that the displacement is below 11 mm and with 99% certainty that the maximum rise of the wellhead during discharge will be 15 mm. This of course depends on the premises of all the input parameters, the model assumptions and limitations, and the assumed load the well is subjected to.

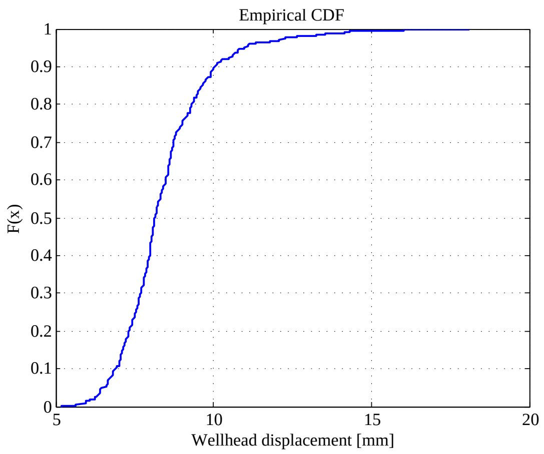

Figure 9: Empirical cumulative distribution function (CDF) plot of the wellhead displacement

Similar statements, as were made to the wellhead movement, can be made to the cumulative distribution function plot of the maximum von Mises stress for the production casing, its surrounding concrete, the anchor casing and its surrounding concrete which are displayed in Figures 10-13. Statistical summary of the output results from the probabilistic analysis is listed in table 4.

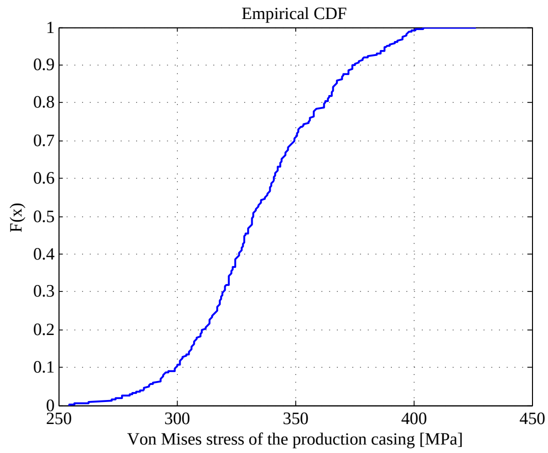

Figure 10: Empirical CDF plot of the maximum von Mises stress in the production casing

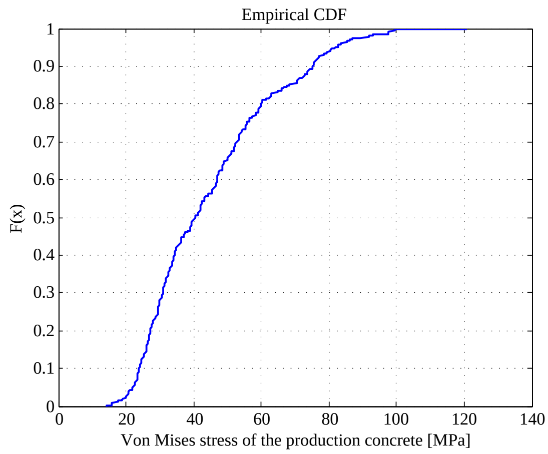

Figure 11: Empirical CDF plot of the maximum von Mises stress in the production concrete

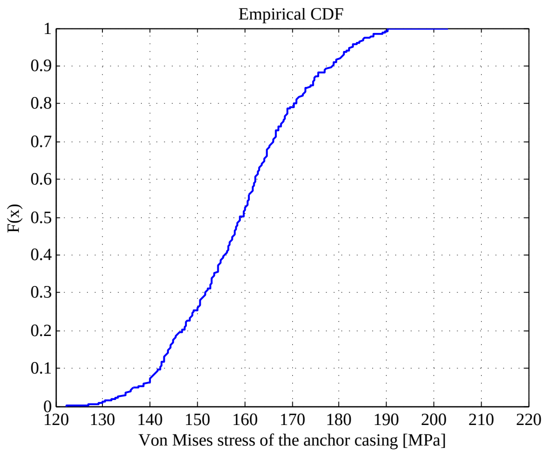

Figure 12: Empirical CDF plot of the maximum von Mises stress in the anchor casing

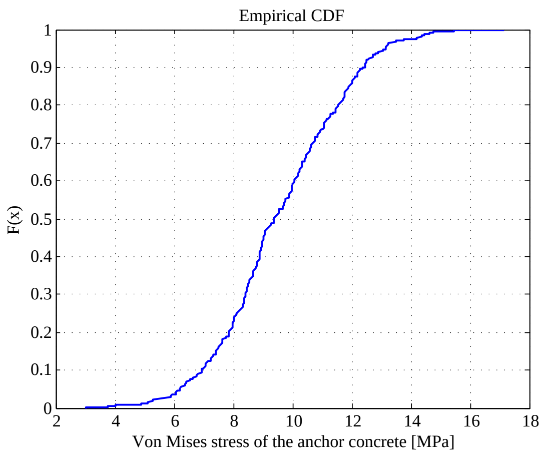

Figure 13: Empirical CDF plot of the maximum von Mises stress in the anchor concrete

Table 4: Statistical summary of the output results from the probabilistic analysis.

	Mean	Std	Min	Max
i.	8.43	1.52	5.19	18.1
ii.	335.6	29.73	254.6	426.5
iii.	44.86	19.55	14.11	120.6
iv.	159.2	13.69	122.3	203.1
v.	9.589	2.163	3.010	17.16

i: Wellhead displacement.

ii: Max. von Mises stress of the production casing.

iii: Max. von Mises stress of the production concrete.

iv: Max. von Mises stress of the anchor casing.

v: Max. von Mises stress of the anchor concrete.

5. Discussion

In the single run of the FEM model it was illustrated how the results appear after 2.5 hours which was the reference time for the probabilistic analysis. The temperature distribution shown in Figure 3 illustrates how shallow the temperature front has reached during this time. Figure 4 illustrates the wellhead displacement and how the production casing slides inside the wellhead. The stress concentration region which is located at the couplings is illustrated in Figures 5 and 6.

The selected outputs of the FEM model for the probabilistic analysis are not as distinctively normally distributed as the input parameters which were randomly given a value within the normal distribution domain. The histograms of the results seen in Figure 8 do however reveal that, apart from the maximum von Mises stress in the concrete surrounding the production casing, the results follow normal distribution nevertheless. The standard deviation given for the input parameters in the probabilistic analysis are intentionally large but might be a bit too spacious. Excluding the insignificant input parameters and narrowing the standard deviation of the significant input parameters should remove some of the noise and improve the results from the probabilistic analysis.

The correlations between input and output parameters reveal which input parameters are significant for each of the output results, see Table 3. Thermal expansion of the casings α_{st} and the parameters for friction, μ_{st} and τ_{max}, proved to be significant to the wellhead displacement, μ_{st} the least significant of the three with a correlation of $R^2 = 0.02528$. Thermal expansion of steel α_{st} is significant for all the selected output results. Specially for the maximum von Mises stress of the production casing and the anchor casing. Scaling the stress-strain curve for steel appears only to be significant for the maximum stress in the production casing and its surrounding concrete sliding freely inside the anchor casing and the wellhead. The anchor casing on the other hand is connected to the wellhead which results in less degree of freedom.

The maximum von Mises stress might not be a good output from the probabilistic analysis since it is a local peak stress which does not resemble the whole casing. Instead or rather additionally, because the maximum is surely of interest, mean stress with standard deviation could be a better option of outputs for comparison.

The cumulative distribution functions (CDF) of the output results, Figures 9 to 13, illustrate the uncertainties of the model. For example it can be stated with 95% certainty and with these premises that the wellhead displacement is below 11 mm, the maximum von Mises stress in the production casing will be lower than 390 MPa, its surrounding concrete 82 MPa, the anchor casing 182 MPa and its surrounding concrete 13 MPa. This means that the production casing has reached beyond the proportional limit of the stress-strain curve for K55 steel which has a minimum yield strength of 379 MPa[3], its surrounding concrete is partially broken, but the security casing and its surrounding concrete are still intact, again with 95% certainty.

6. Conclusion

In this paper, probabilistic analysis of a structural FEM model of a high temperature geothermal well was presented. Using probabilistic methods on FEM models provide a broader understanding of the problem and the model itself and produce a topography of the results as well as enabling the uncertainties of the model to be quantified.

7. Acknowledgment

This work was supported by the University of Iceland research fund, the Technology Development Fund at RANNIS - The Icelandic Center for Research, the Innovation Center Iceland, Landsvirkjun Energy Research Fund, and GEORG - Geothermal Research Group. Their support is much appreciated.

Nomenclature

E	Young's modulus
E_{st}	Young's modulus of steel
E_{co}	Young's modulus of concrete
E_{gr}	Young's modulus of formation
ν	Possion's ratio
ρ	Density
ρ_{st}	Density of steel
ρ_{co}	Density of concrete
fc	Compressive strenght of concrete
K	Thermal conductivity
c	Specific heat
α	Thermal expansion
α_{st}	Thermal expansion of steel
α_{co}	Thermal expansion of concrete
μ	Coefficient of friction
τ_{max}	Maximum shear stress
τ_{lim}	Limit shear stress
τ	Equivalent shear stress
P	Contact normal pressure
b	Contact cohesion
R^2	Coefficient of determination
σ	Standard deviation
σ-ϵ_{sc}	Stress-strain curve scaling factor

References

[1] *Release 14.5 documentation for ANSYS*, 2012.

[2] Robert D. Cook, David S. Malkus, Michael E. Plesha, and Robert J. Witt. *Concepts and Applications of Finite Element Analysis*. John Wiley & Sons, Inc, 111 River Street, Hoboken, NJ 07030, 2002.

[3] Gilles Gabolde and Jean-Paul Nguyen. *Drilling Data Handbook*. IFP publications, Éditions Technip, 27 rue Ginoux, 75737 Paris Cedex 15, France, 2006.

[4] S. Gretarsdottir. Mechanical and thermal properties of well cement. Master's thesis, University of Iceland, 2007.

[5] Hagen Hole. Geothermal well design - casing and wellhead. *Petroleum Engineering Summer School*, June 2008. Workshop 26.

[6] Gunnar Skúlason Kaldal. Load history and buckling of the production casing in a high temperature geothermal well. *Thirty-Sixth Workshop on Geothermal Reservoir Engineering, Stanford University, Stanford, California*, february 2011.

[7] Gunnar Skúlason Kaldal. Thermal and structural analysis of the casing in a high temperature geothermal well during discharge. *Thirty-Seventh Workshop on Geothermal Reservoir Engineering, Stanford University, Stanford, California*, february 2012.

[8] Gunnar Skúlason Kaldal. Collapse analysis of the casing in high temperature geothermal wells. *Thirty-Eighth Workshop on Geothermal Reservoir Engineering, Stanford University, Stanford, California*, february 2013.

[9] S. N. Karlsdottir and I. O. Thorbjornsson. High Temperature Geothermal Wells - Center of Excellence in Iceland - Phase I: Corrosion Testing of Steel in High Temperature Geothermal Wells in Iceland. Technical Report for RANNIS (The Icelandic Centre for Research), October 2009.

[10] L. Magnusdottir. Nonlinear finite element model of a geothermal well. Master's thesis, University of Iceland, 2009.

[11] A. Ragnarsson. Utilization of Geothermal Energy in Iceland. *International Geothermal Conference, Reykjavik, Iceland*, pages 39–45, September 2003.

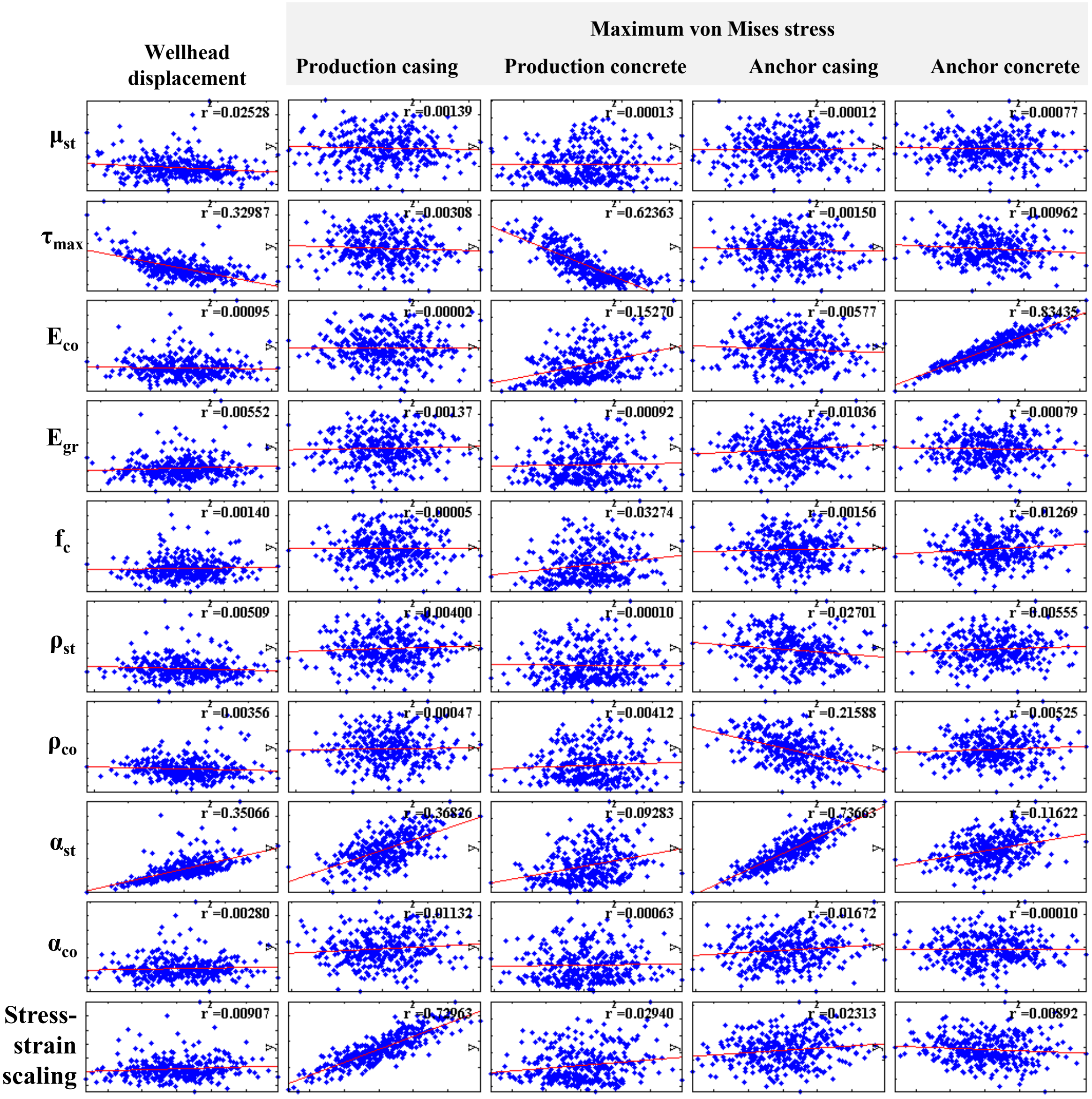

Figure 14: Correlation between selected input parameters and results.